The Journal of Experimental Biology 210, 946-955
Published by The Company of Biologists 2007
doi:10.1242/jeb.001800

The major vault protein is related to the toxic anion resistance protein (TelA) family

Kathy A. Suprenant[1,*], Nathan Bloom[1], Jianwen Fang[2] and Gerald Lushington[3]

[1]*Department of Molecular Biosciences, University of Kansas, Lawrence, KS 66045, USA,* [2]*Bioinformatics Core Facility and* [3]*Molecular Graphics and Modeling Laboratory, University of Kansas, Lawrence, KS 66045, USA*

*Author for correspondence (e-mail: ksupre@ku.edu)

Accepted 10 January 2007

Summary

Vaults are barrel-shaped ribonucleoprotein particles that are abundant in certain tumors and multidrug resistant cancer cells. Prokaryotic relatives of the major vault protein, MVP, have not been identified. We used sequence analysis and molecular modeling to show that MVP and the toxic anion resistance protein, TelA of *Rhodobacter sphaeroides* strain 2.4.1, share a novel fold that consists of a three-stranded antiparallel β-sheet. Because of this strong structural correspondence, we examined whether mammalian cell vaults respond to tellurite treatment. In the presence of the oxyanion tellurite, large vault aggregates, or vaultosomes, appear at the cell periphery in 15 min or less. Vaultosome formation is temperature-dependent, reversible, and occurs in normal human umbilical vein endothelial cells as well as transformed HeLa cervical cancer cells. Vaultosome formation is not restricted to tellurite and occurs in the presence of other toxic oxyanions (selenate, selinite, arsenate, arsenite, vanadate). In addition, vaultosomes form independently from other stress-induced ribonucleoprotein complexes, stress granules and aggresomes. Vaultosome formation is therefore a unique cellular response to an environmental toxin.

Key words: protein structure, ribonucleoproteins, terratogens, toxins fluorescent antibody technique, indirect and computational molecular biology.

Introduction

Vaults are large, hollow ribonucleoprotein particles that are conserved from *Dictyostelium* to humans (Kedersha et al., 1986). To date, no prokaryote relatives of the vault particle have been identified. The barrel-shaped vault complex comprises the major vault protein (MVP), telomerase-associated protein-1 (TEP1) and the vault poly(ADP-ribose) polymerase (VPARP), and an untranslated small RNA (Suprenant, 2002). The major vault protein (MVP) comprises 75% of the mass of the vault particle and expression of MVP in baculovirus-infected insect cells is sufficient to self-assemble into a vault-like particle with the same overall shape and dimensions of the native vault structure (Stephen et al., 2001). Surprisingly, these vault shells are very dynamic and are capable of 'breathing' to allow the incorporation of TEP1, VPARP and potential cargo molecules (Poderycki et al., 2006).

The function of vaults remains elusive. High levels of vaults are correlated with a poor prognosis in certain cancers and with some multi-drug resistant (MDR) cancer cell lines (Scheffer et al., 2000). Although most vaults reside in the cytosol, a small but detectable fraction (~5%) is associated with the nucleus and it has been suggested that vaults may be involved in nucleocytoplasmic transport (Chugani et al., 1993; Hamill and Suprenant, 1997; Slesina et al., 2005; Stewart et al., 2005; van Zon et al., 2006). MVP may act as a scaffolding protein for the protein tyrosine phosphatase, SHP-2 and activated extracellular-regulated kinases (ERKs) (Kolli et al., 2004). In addition to interacting with the epidermal growth factor signaling pathways, MVP expression is upregulated through the JAK/STAT signaling pathway (Steiner et al., 2006).

From molecular analyses and high-resolution cryoelectron microscopy, we know that vault composition and structure are highly conserved (Kedersha et al., 1990; Kong et al., 1999; Mikyas et al., 2004; Stewart et al., 2005). The primary sequence of MVP comprises seven short repeats of ~55 amino acids at the amino terminus, a central region and a coiled-coil interaction domain at the carboxyl terminus (van Zon et al., 2002), as depicted schematically in Fig. 1A. The repeat unit (aa 26–401) is highly conserved across eukaryotes and forms the basis for a characteristic protein sequence domain. The solution NMR structure of a two-repeat domain of the MVP reveals that the walls of the central barrel are built from repeating units of a unique three-stranded anti-parallel sheet (Kozlov et al., 2006). This structural repeat is the same length as the sequence repeat but is shifted by half of a sequence repeat (~26 amino

acids). The coiled-coil domain at the C terminus is thought to align the MVPs at the vault cap (Kozlov et al., 2006; Mikyas et al., 2004; van Zon et al., 2002).

Eukaryotic MVP coding sequences are well represented in the public databases. To date, MVP sequences have been identified in birds, mammals, amphibians, bony fishes, rays, echinoderms, mollusks, flatworms and trypanosomatids. Recognizable MVP sequences are notably absent in the genomes of *C. elegans*, *D. melanogaster* and *S. cerevisiase*. In this study, we initiated a sequence-based approach to understanding vault function. We report that the major vault protein (MVP) is related to the toxic anion-resistance protein, TelA, of *Rhodobacter sphaeroides* strain 2.4.1 and that mammalian MVP responds dynamically to tellurite, and other toxic oxyanions. We propose that vaults are an unrealized component of a stress response pathway that originated in bacteria.

Materials and methods

Sequence and structure analysis

Prospective homologs to MVP were initially identified by subjecting the MVP repeat sequence to an iterative search of the non-redundant protein sequence database (National Center for Biotechnology, NIH Bethesda, MD, USA) using the PSI-BLAST program (Altschul and Koonin, 1998). The second search iteration yielded the tellurite resistance protein (TelA) from *Rhodobacter sphaeroides* (AF019377) as a plausible match (homologous alignment with E=6e–15). Based on the results of our initial BLAST search for homologs to the MVP repeat unit in which TelA was identified, we performed a reciprocal search based on the sequence of tellurite resistance protein, retrieving the eukaryotic MVP in a second round of iteration (E<3e–8). Further analysis of the eukaryotic MVP domain in common with the toxic ion resistance proteins revealed that the highest degree of similarity was found in a large internal repeat (residues 103–221; 156–276). An iterative search with this internal repeat (103–221) also identified the tellurite resistance protein (E=2e–14).

Having identified internally consistent evidence for homology between the eukaryote MVP repeat and TelA, a sequence alignment of two was carried out using the ClustalW program (Thompson et al., 1994) with the BLOSUM-30 substitution matrices (permitting both positive and negative match scoring) (Henikoff and Henikoff, 1992), a gap-opening penalty of 10 and a gap-extension penalty of 0.1. The portion of the sequence corresponding to the MVP domains 3 and 4 resolved *via* NMR (Kozlov et al., 2006) yielded a net identity score of 31% relative to TelA, and a similarity score of 56%. These scores would normally suggest a probable homologous (potential superfamilial) relationship and a reasonable probability of a conserved domain 3/4 fold, but further scrutiny of the computed alignment relative to the three-dimensional structure revealed unphysical gaps within key MVP beta strands that would preclude common folding. Intuitive manipulation of the alignment to preferentially shrink gaps within strands at the expense of known coil regions, however, led to formulation of an alternative sequence alignment, reported in Fig. 1B, that retains 30% TelA identity and 55% similarity relative to the domain 3/4 region of MVP. This alignment meets the basic minimum criterion for meaningful homology modeling (~30% sequence identity), and appears to be physically reasonable, thus we used it as the basis for comparative structure prediction for the portion of TelA in alignment with MVP domains 3 and 4. The TelA model was then constructed v*ia* the Modeller program (Marti-Renom et al., 2000). Default restraint settings were retained, and rigorous simulated annealing steps using the Chemistry at HARvard Molecular Mechanics (CHARMM) force field and charges (MacKerell, Jr et al., 1998) were employed in order to permit reasonable relaxation of the 12-residue TelA loop (MQSLPSIRLVQE), for which no MVP template residues exist. Specifically, five simulated annealing cycles of 4.4 ps stepwise warming (0 K→150 K→250 K→400 K→700 K→1000 K) followed by 19.2 ps stepwise cooling (1000 K→800 K→600 K→500 K→400 K→300 K) were performed. The resulting structure was then examined for unrealistic contacts and geometry *via* the ProCheck program (Laskowski et al., 1993). Further structural analysis on the proteins was carried out using the SYBYL suite of programs (Tripos, 2006).

Antibodies

The primary antibodies used in this study were: anti-β-tubulin antibody Tub2.1 (Sigma-Aldrich, St Louis, MO, USA), anti-MVP antibody LDQN (Eichenmuller et al., 2003), anti-VPARP antibody ACE (a kind gift of Valerie Kickhoefer, David Geffen School of Medicine at UCLA, Los Angeles, CA, USA) (Kickhoefer et al., 1999), anti-PABP antibody 10E10 (a kind gift of Gideon Dreyfuss, University of Pennsylvania, School of Medicine, Philadelphia, PA, USA) (Gorlach et al., 1994), anti-HnRNPA2 antibody EF67 (a kind gift of William Rigby, Dartmouth Medical School, Lebanon, NH, USA) (Nichols et al., 2000), anti-TIA-1 3E6 (a kind gift of Nancy Kedersha, Brigham and Women's Hospital, Boston, MA, USA) (Taupin et al., 1995) and anti-ubiquitin antibody FK-2 (StressGen Biotechnologies, Ann Arbor, MI, USA).

Cell culture

HeLa cervical cancer cells (ATTC CCL-2) and human umbilical vascular endothelial cells (HUVEC; ATCC CRL-1730), were grown in T-75 tissue culture flasks in Dubecco's Modified Eagle's Medium (DMEM)/Hams F12 supplemented with 2 mmol l^{-1} L-glutamine, 10% fetal bovine serum, 100 units ml^{-1} penicillin and 100 μg ml^{-1} streptomycin. HeLa cells used in MVP siRNA knockdown assays were cultured in DMEM containing 4 g l^{-1} glucose and supplemented with 4 mmol l^{-1} glutamine, 10% fetal bovine serum (FBS), 500 units ml^{-1} penicillin, 0.1 mg ml^{-1} streptomycin and 0.01 mg ml^{-1} of Tylosin. HUVEC culture medium additionally contained 15 μg ml^{-1} endothelial cell growth supplement (Biomedical Technologies, Inc., Stoughton, MA, USA) and 100 μg ml^{-1} heparin. The culture flasks for the HUVECs were

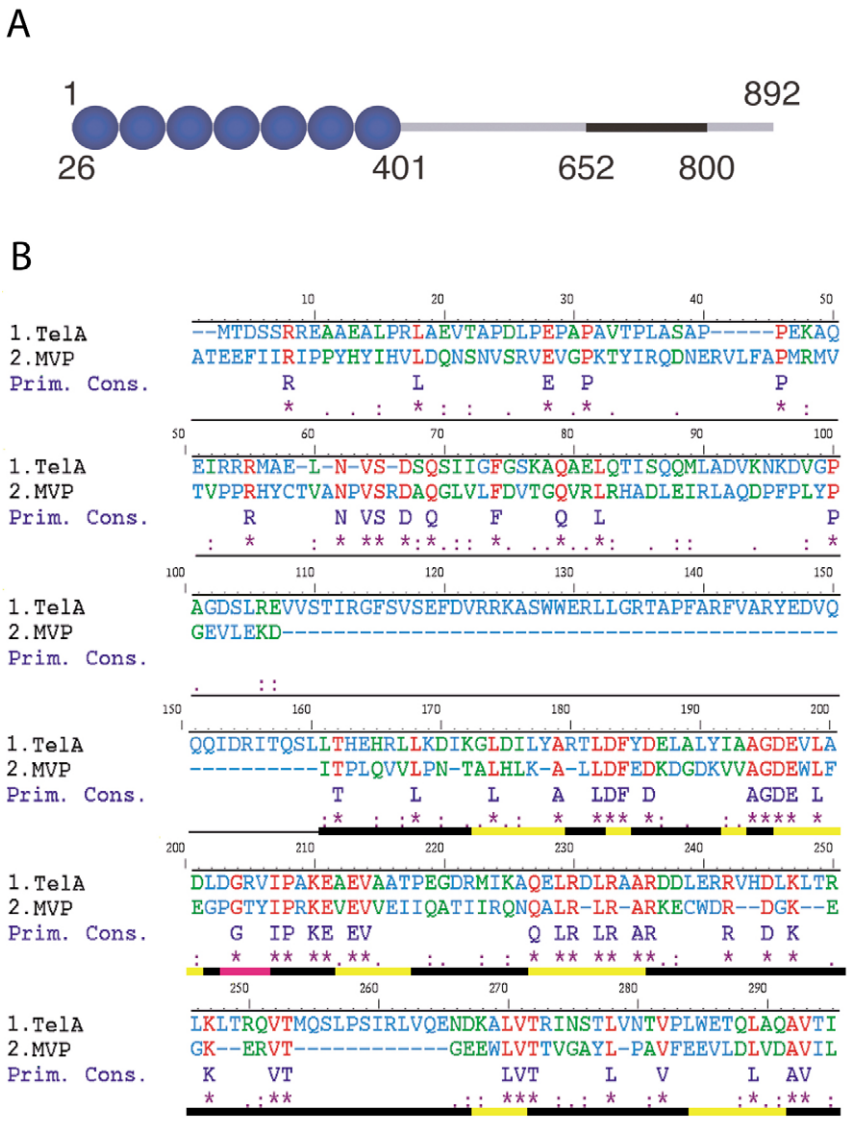

Fig. 1. Sequence similarity between the mammalian major vault protein (MVP) and the bacterial tellurite resistance protein (TelA). (A) Schematic diagram of the major vault protein (MVP). Human MVP is composed of an amino-terminal domain (aa 26–401) comprising a series of seven imperfect repeats (blue circles) and a carboxyl-terminal region (black bar) that contains a coiled-coil domain (aa 652–800). (B) Sequence alignment of the repeat unit of MVP with TelA. Residue number corresponds to the consensus gapped sequence and thus does not correspond perfectly to that of either constituent sequence. Amino acid symbols are colored according to quality of match, with red indicating perfect conservation (redundantly labeled with a asterisk in the bottom line), green indicating substantial similarity (colon, strong similarity; stop, moderate similarity) and light blue indicating a mismatch. The line labeled 'Prim. Cons.' reports known residues within the consensus sequence (dark blue script). The portion of the MVP sequence structurally resolved in NMR studies (Kozlov et al., 2005) is underlined with a bar colored according to observed secondary structure: magenta for helices, yellow for beta strands, and black for coils and turns.

coated with type-1 rat-tail collagen. All cells were maintained in an atmosphere with 5% CO_2 at 37°C, unless otherwise noted.

Immunofluorescence microscopy

Adherent cells were detached from the flasks by a 5 min incubation (37°C) with a trypsin-EDTA solution (0.01% crystalline trypsin, 0.1% EDTA in divalent-cation-free Dulbecco's PBS). The cells were washed once with medium containing 5% FBS, diluted, seeded onto coverslips and grown for 24 h at 37°C. Cells were treated with either potassium tellurite (K_2TeO_3), sodium selenite (Na_2SeO_3), sodium selenate (Na_2SeO_4), sodium arsenite (Na_3AsO_3), sodium arsenate (Na_3AsO_4) or sodium orthovandate (Na_3VO_4), as described in the Results, and fixed with either –20°C methanol for 5–7 min or 2–4% paraformaldehyde for 15 min. No differences were observed in the staining patterns for the anti-vault antibodies with either fixation procedure so methanol fixation was used throughout the studies reported. The cells were rinsed three times with PBS and incubated with the primary antibodies for 60 min at 37°C. After rinsing the coverslips four times (10 min each rinse) with PBS, the cells were incubated with either Cy3- or Cy2-conjugated secondary antibodies (Jackson ImmunoResearch Laboratories, West Grove, PA, USA). The coverslips were rinsed three times with PBS and once with 300 nmol l^{-1} 4′,6-diamidino-2-phenylindole (DAPI) in PBS to counterstain the nuclei. The coverslips were mounted in 90% glycerol and 10% PBS, pH 9.0 containing 4% (w/v) *n*-propyl gallate. Images were acquired by using a Nikon Optiphot microscope equipped with a Zeiss 63X, 1.3 NA objective lens and an Orca ER cooled CCD camera (Hamamatsu, Bridgewater, NJ, USA). Image acquisition was controlled by OpenLab software (Improvision, Inc., Lexington, MA, USA) and compiled using Adobe Photoshop.

Results

Prokaryotic relatives of the major vault protein (MVP)

In addition to verifying a potential homologous relationship between the MVP repeat unit and TelA, our reciprocal BLAST search retrieved several toxic ion resistance proteins from *Staphlococcus aureus*, *Bacillus subtilis*, *Listeria monocytogenes*, *Clostridium acetobutylicum* and *Streptococcus pyogenes* (first round of iteration, E<2e–6). As well, a detailed sequence comparison *via* the PROSITE database (Hulo et al., 2004) indicates that both the MVP repeat segment and its putative TelA homolog display extensive and reasonably

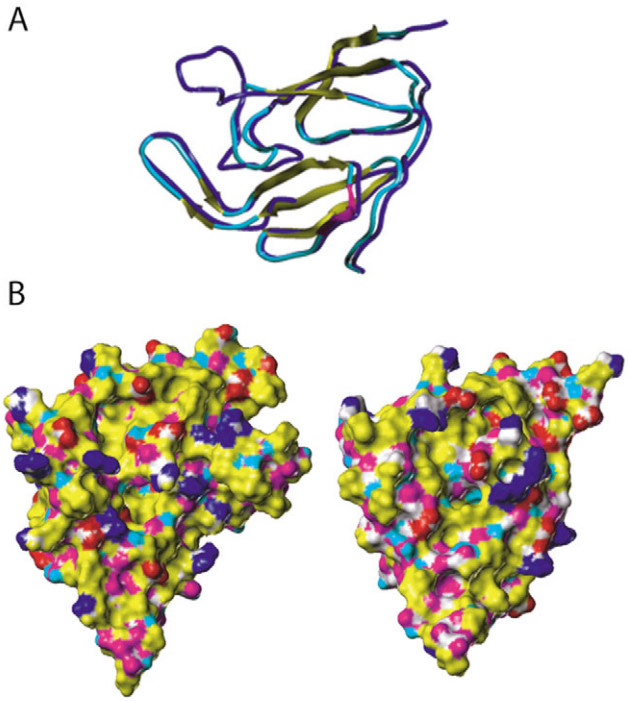

Fig. 2. Relative structures of our model for the TelA protein and its associated MVP template, shown as (A) overlapping ribbon diagrams and (B) juxtaposed solvent accessible surfaces for TelA (left) and MVP (right). Ribbon coloring of MVP in A corresponds to observed secondary structure elements: magenta=helices, yellow=beta strands/sheets, cyan=coils/turns, while for contrast the TelA backbone is rendered as a monochromatic blue tube. Surface rendering in B reflects relative electrostatics, with the following color scheme: N,H portions of cationic side chains are blue, anionic carbonyl oxygens are red, other neutral H-bond acceptor atoms are magenta, donatable protons are cyan, polar aliphatic groups are white and all hydrophobic groups are yellow.

strong similarity (greater than 60%) with S-layer paracrystalline bacterial surface coatings. These findings strongly suggest that aspects of mammalian MVP are more closely related to a variety of prokaryotic proteins, strongly bolstering the plausibility for a common ancestry between the eukaryotic MVP and TelA.

TelA structure prediction

The highly similar spatial alignment of TelA and MVP shown in Fig. 2A, even after fairly thorough simulated annealing of the former, suggests that the fold exhibited by MVP is likely a viable conformation for TelA. Incorporation of an additional 12 residues of TelA (MQSLPSIRLVQE) into the coil between the 4th and 5th strands of the MVP sheet structure does not appear to impose substantial new strain within the TelA structure. In fact, ProCheck analysis (Laskowski et al., 1993) suggests that our predicted TelA structure may be under less strain (only nine bad atomic contacts flagged) than the MVP template itself (20 bad contacts) on which the TelA model was based, perhaps due to explicit solvent effects on the latter NMR structure. Otherwise, ProCheck analysis provided a comparable assessment of the physical soundness of both structures, determining an average G-factor score (accounting for all torsions, bond angles and bond distances) of –0.50 for MVP and –0.48 for TelA, both of which are well within the acceptable range.

An indication of the relative size, shape and surface charge distribution of our predicted TelA model and its MVP template is given in Fig. 2B. Given the fact that the portion of the TelA sequence corresponding to domains 3,4 of MVP resolved *via* NMR is longer by 22 amino acids (135 *vs* 113), it is not surprising that the predicted TelA volume (28 212 $Å^3$) and surface area (9083 $Å^2$) are somewhat larger than that computed for MVP (24 096 $Å^3$ and 7954 $Å^2$, respectively). This is reflected in a marginally larger appearance in the rendered versions in Fig. 2B. The shape of the two proteins, however, is very similar, with the only major difference between the two being an additional lobe just below the upper right corner of the TelA structure, corresponding to the aforementioned unmatched 12 residues between the 4th and 5th strands of the sheet structure. This extended coil is located mostly on the surface of the TelA structure, which suggests that it is unlikely to significantly perturb the basic fold of the protein relative to MVP, but may yield modest differences in protein-protein associative tendencies, environmental preferences, and functionality. Beyond this, however, the two systems have very similar electrostatic/hydrophobic profiles, with polar residues constituting 41.7% of the MVP and 40.5% of the TelA surface areas. It is interesting to note, however, that while MVP has only a modest difference in the relative surface areas of cationic and anionic residues (1264 and 1185 $Å^2$, respectively), the ratio is significantly more slanted toward surface cations in the case of TelA (1531 *vs* 1047 $Å^2$).

MVP aggregates form in response to tellurite

We investigated whether MVP abundance or cellular location changed in response to tellurite treatment. Previously, we generated an antipeptide antibody (anti-LDQN), against conserved sequences within the amino terminus of the MVP, and showed that MVP localizes predominantly to the cytosol in a punctate staining pattern (Eichenmuller et al., 2003). In the HeLa cytosol, MVP is concentrated near the nucleus where the cell is the thickest (Fig. 3A). In addition, unidentified intranuclear speckles are also observed with this anti-MVP antibody. As you move outwards towards the cell periphery the number of MVP puncta diminishes. A similar staining pattern has been described with other MVP antibodies (Kedersha et al., 1990; Kickhoefer et al., 1999; van Zon et al., 2003). When potassium tellurite (K_2TeO_3) is added to the culture medium, MVP is no longer concentrated near the nucleus. In contrast, MVP is found in large, irregularly shaped cytoplasmic aggregates. In some cases, the aggregates are as large as 7 μm in diameter. The MVP aggregates are found predominantly at the cell margins where the cell makes contact with the substrate. Aggregate formation is temperature sensitive and can

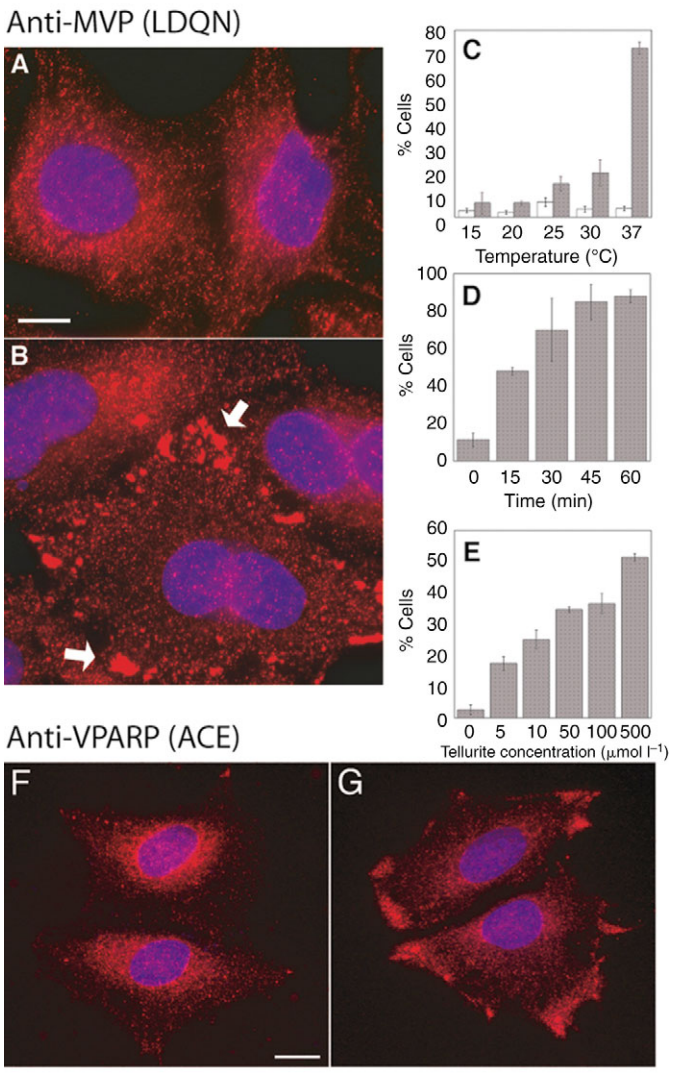

Fig. 3. MVP and VPARP accumulations in the presence of tellurite. (A) Fluorescence micrograph of an untreated HeLa cell stained with an antibody against the major vault protein (LDQN) (red) and counterstained with DAPI. Bar, 10 μm. (B) Pronounced MVP aggregates (arrows) are revealed when HeLa cells are grown at 37°C for 30 min in the presence of 0.5 mmol l^{-1} K_2TeO_3. (C) The formation of MVP aggregates is temperature dependent. HeLa cells were cultured at 37°C and then incubated in the presence (filled bars) and absence (open bars) of 0.5 mmol l^{-1} K_2TeO_3 for 30 min at the temperatures shown. The number of cells with MVP aggregates (approximately 2 μm or larger) were counted and expressed as a percentage of the total cells. At least 100 cells were examined at each temperature and the experiment was done in triplicate. Values are reported as mean % ± s.d. (D) The percentage of cells with MVP aggregates increases over a 1 h incubation. HeLa cells were incubated in the presence of 0.5 mmol l^{-1} K_2TeO_3 for 30 min and the percent of cells with aggregates were quantified as described above. (E) Nearly 20% of the HeLa cells incubated in 5 mmol l^{-1} K_2TeO_3 will form MVP aggregates. The higher the concentration of K_2TeO_3, the greater the percentage of HeLa cells with MVP aggregates. (F) Fluorescence micrograph of untreated HeLa cells stained with an antibody against the vault-associated poly(ADP-ribosyl)polymerase (VPARP) and counterstained with DAPI. Bar, 10 μm. (G) VPARP accumulations also appear at the cell periphery during a 30 min incubation in the presence of 0.5 mmol l^{-1} K_2TeO_3.

occur in 15 min or less and at tellurite concentrations as low as 5 μm.

As mentioned above, nearly all the MVP in the cell is assembled into a vault particle (Kickhoefer et al., 1999; Siva et al., 2001). Therefore it is likely that vault particles move to the cell margins in response to tellurite treatment. To be certain that this is indeed the case, tellurite-treated cells were immunostained with a polyclonal antibody against the vault-associated poly(ADP-ribose) polymerase (VPARP). VPARP catalytically adds ADP-ribose polymers to itself and MVP and is located in three stave-like bands on the inside of the vault barrel (Kickhoefer et al., 1999; Mikyas et al., 2004). In HeLa cells, anti-VPARP antibodies stain peri-nuclear cytoplasmic puncta as well as intranuclear speckles (Kickhoefer et al., 1999) (Fig. 3F). In the presence of tellurite, VPARP staining occurs in large aggregates at the cell periphery (Fig. 3G). Since MVP and VPARP are integral components of vaults, it is likely that the peripheral accumulations of VPARP and MVP occur together in an intact vault particle. We refer to these large vault aggregates as vaultosomes.

Vaultosomes form at the cell margins in non-transformed endothelial cells

Since HeLa cells are derived from an aggressive glandular cervical cancer, it is important to determine whether vaults respond to tellurite treatment in a non-transformed cell line. For these experiments, we examined vault location in HUVEC cells, an endothelial cell line derived from normal human umbilical cord. In untreated HUVEC cells, MVP is concentrated in the cytosol near the nucleus in a pattern that is indistinguishable from that seen in the aneuploid HeLa cell line (Fig. 4A). Upon tellurite exposure, MVP staining appears to be concentrated at the cell periphery in irregularly shaped patches or aggregates (Fig. 4B). Thus, vaults respond to tellurite in a similar manner in these two different human cell lines.

The formation of vaultosomes is reversible

Exposure to 0.5 mmol l^{-1} tellurite for 30 min does not affect cell viability (Ding et al., 2002). HeLa cells were exposed to 0.5 mmol l^{-1} tellurite for 30 min, washed with fresh medium and allowed to recover in tellurite-free medium overnight. Over a 24 h period, the cell number had doubled in both the tellurite-treated and untreated cultures (compare Fig. 4E with H). In addition, the vaultosomes were no longer present at the cell margins. The MVP staining pattern in the tellurite-treated and recovered cells was identical to the untreated cells (compare Fig. 4C with E). These experiments lead us to conclude that vaultosome formation is a dynamic and reversible process.

Tellurite does not depolymerize the microtubule cytoskeleton

Previous studies have shown that vaults bind directly to microtubules *in vivo* and *in vitro* (Eichenmuller et al., 2003;

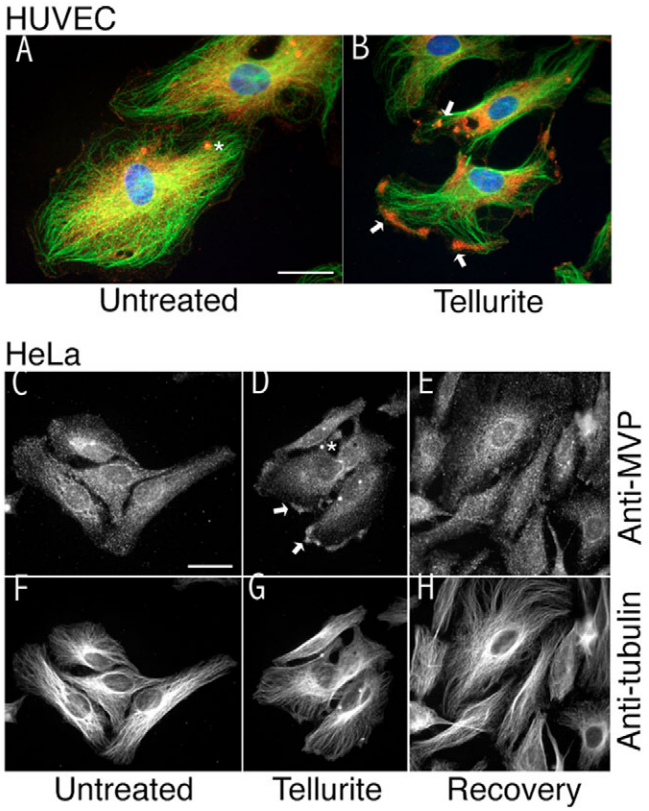

Fig. 4. Vault aggregation in normal normal human vascular endothelial cells (HUVECs) and the HeLa cancer cell line. HUVECs were incubated at 37°C for 30 min in the presence (A) or absence (B) of 0.5 mmol l^{-1} K_2TeO_3 and subsequently stained with antibodies against MVP (red) and tubulin (green). MVP aggregates form at the cell periphery in HUVECs (arrows). In addition, HeLa cells were incubated at 37°C for 30 min in the presence or absence of 0.5 mmol l^{-1} K_2TeO_3 and subsequently stained with tubulin and MVP antibodies (C–G). HeLa cells were subsequently washed three times in fresh medium without tellurite and incubated for an additional 24 h, fixed and processed for immunofluorescence. Accumulation of MVP at the cell periphery of HeLa cells is reversible. The MVP aggregates at the cell periphery (arrows, D) in the tellurite-treated cells are absent after a 24-h recovery period (E). In addition, the cell number has doubled in both the treated and untreated cultures. Occasionally, brightly-staining puncta form in response to tellurite treatment (asterisks). These bright MVP puncta are different from the MVP aggregates at the cell periphery in that these puncta stain with both MVP and tubulin. Bar, 20 μm.

Hamill and Suprenant, 1997). To be certain that vault aggregation at the cell margin was not dependent upon microtubule reorganization or depolymerization, the cells shown in Fig. 4 were double stained with antibodies against tubulin and MVP. In untreated HeLa and HUVEC cells, the microtubules extend radially from the mitotic organizing center near the nucleus to the cell periphery. Exposure to tellurite did not have a great effect on the organization of the HeLa cell microtubules (compare Fig. 4F with G). In the HUVECs, the microtubule array also extends radially from the nucleus to the cell surface although the microtubules are somewhat collapsed in regions where the cells lost their attachment to the coverslips. Tellurite appears to be more toxic to the HUVECs. Even so, the vaults were still aggregated at the cell periphery (Fig. 4B). These experiments indicate that a catastrophic change in the microtubule array was not responsible for the tellurite-induced movement of vaults to the cell margin.

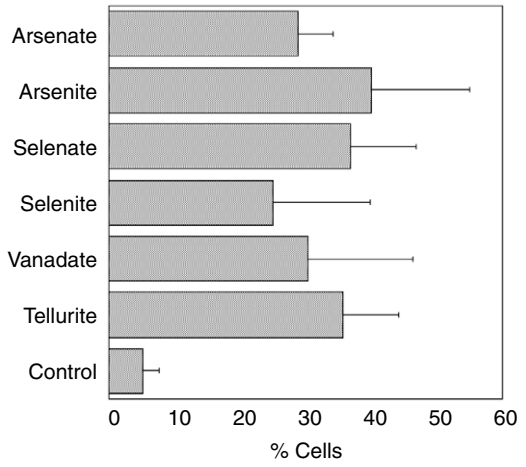

Fig. 5. Bar graph showing the percentage of cells with vaultosomes following a 15 min treatment with 0.5 mmol l^{-1} arsenate, arsenite, selenate, selenite, vanadate and tellurite. Experiments were done in triplicate; values are means ± s.d.

Vaultosome formation in the presence of other oxyanions

To determine whether the response was specific to tellurite, HeLa cells were treated with sodium arsenite, sodium arsenate, sodium orthovanadate, sodium selenite, sodium selenate or potassium tellurite (all at 0.5 mmol l^{-1}, 15 min, 37°C), fixed and examined by immunofluorescence. Vaultosomes formed in the presence of all of these oxyanions, albeit to different extents ranging from 25 to 40% of the cells examined (Fig. 5). Cells treated with arsenite are more likely to contain vault aggregates although differences amongst the various ions are not statistically significant. Moreover, the MVP aggregates found in cells treated with arsenite or tellurite appear brighter by immunofluorescence than the MVP aggregates found in cells treated with selenite, selenate or vanadate, for example.

Vaultosomes do not form during a general stress response. To determine whether vault aggregation was a general stress response, HeLa cells were heat-shocked (44°C, 60 min) or UV irradiated (100 μJ) and the location of the MVP was monitored by immunofluorescence. Similar to a previous study (Kickhoefer et al., 1999), no changes in the distribution of the MVP were observed with either treatment (data not shown).

Vaultosomes form independently of other ribonucleoprotein complexes

Arsenite is known to inhibit protein synthesis and to accumulate untranslated RNAs into dense stress granules (Anderson and Kedersha, 2002). Since the vaultosomes also

formed under toxic ion stress, we reasoned that the vaultosomes might be large enough to harbor the stress granules. To examine whether stress granules were associated with vaultosomes, we treated cells with arsenite and immunostained the cells with antibodies against vaults and the RNA-binding protein TIA-1, a robust marker of mammalian stress granules (Kedersha et al., 1999). Arsenite treatment induced the formation of vaultosomes and the smaller stress granules; however, neither particle colocalized with each other in the cell (Fig. 6). Furthermore, vaultosome formation was not affected by drugs (emetine, puromycin) that affect the dynamic equilibrium of RNAs in the stress granules (Kedersha et al., 2000) (data not shown). These results indicate that vaultosomes form independently of stress granules.

To examine whether other RNPs were associated with the vaultosomes, we treated cells with arsenite and immunostained the cells with antibodies against either the mRNA polyA-binding proteins-I (PABP-I) or the heterogeneous nuclear ribonucleoprotein A2, a protein implicated in translational regulation, RNA processing and RNA transport (Dreyfuss et al., 1993; Hamilton et al., 1999; Kwon et al., 1999). Neither RNA binding protein, PABP-I or hnRNP A2 appear to colocalize to a significant extent with the vaults in untreated cells or arsenite-induced vaultosomes (data not shown).

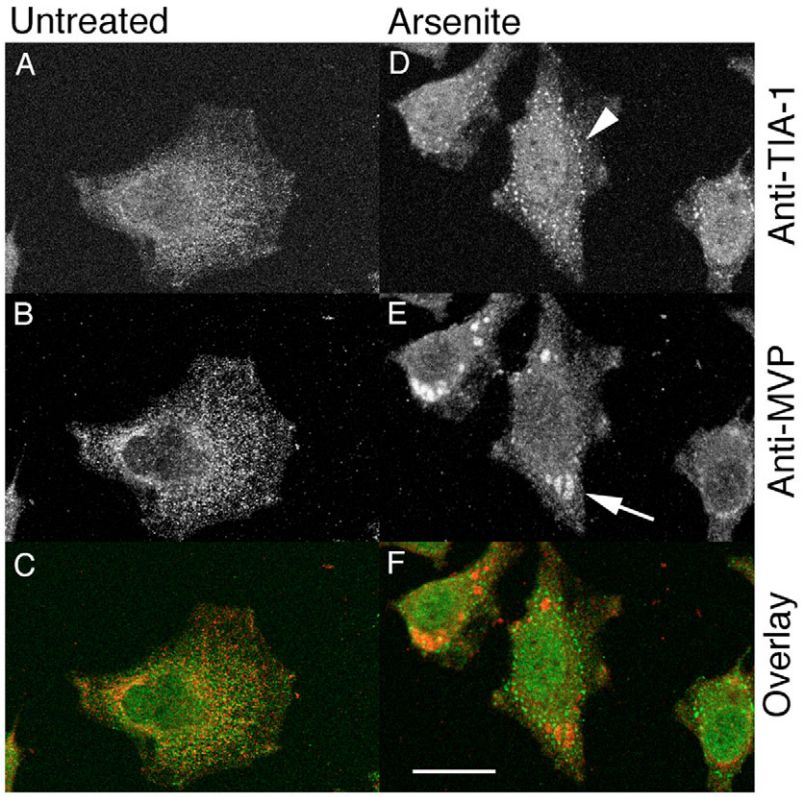

Fig. 6. Mammalian stress granules and vaultosomes do not colocalize. HeLa cells were incubated with 0.5 mmol l^{-1} sodium arsenite for 15 min at 37°C (D–F) or left untreated (A–C). Fluorescence micrographs show HeLa cells stained with antibodies against the RNA-binding protein TIA-1 (A,D) or MVP (B,E). Three-color overlays are shown in C and F. Vaultosomes (arrowhead in D) do not colocalize with TIA-1 proteins. Bar, 20 μm.

Vaultosomes are not aggresome-like

In response to proteosome inhibition, aggregates of ubiquinated proteins and proteosome subunits will accumulate around the microtubule organizing center of HeLa cells (Wojcik et al., 1996). These 'aggresomes' form when the synthesis of misfolded proteins exceeds the capacity of the chaperones and the proteosomes (Johnston et al., 1998). We examined whether vaultosomes colocalized with ubiquinated proteins in the aggresomes when cells are treated with the proteosome inhibitor, N-acetyl-Leu-Leu-Norleucinal (ALLN). Fig. 7 shows that aggregates of ubiquinated proteins are found near the nucleus of the HeLa cells after treatment with ALLN. We were surprised to find that vaults also aggregated when the HeLa cells were treated with ALLN, however the vaultosomes did not colocalize with the ubiquinated proteins in the aggresomes. These results show that vaultosomes form in response to proteosome inhibition; however, vaultosomes do not colocalize with the aggresomes.

Discussion

Biological effects of tellurium and tellurite

Elemental tellurium (Te), named from the Latin 'tellus' meaning 'earth', was discovered by F. J. Mueller von Reichenstein in 1782 from ores mined in the gold districts of Transylvania (Cooper, 1971). In humans, elemental tellurium is very toxic and induces both chronic and acute toxicity, with death being the most extreme outcome. Although the toxic metalloid tellurium is relatively rare in the natural environment, several electrical, metallurgical and chemical manufacturing applications generate elevated levels of tellurium in the environment.

The toxicology of tellurium compounds on humans and other animals has been studied in detail, but the basic mechanism(s) of cellular toxicity is not known. For example, one of the earliest documented biological effects of tellurium poisoning is the demyelination of the sciatic nerve due to the inhibition of cholesterol biosynthesis and the accumulation of squalene in Schwann cells (Harry et al., 1989; Lampert et al., 1970). In bacteria, the toxicity of the soluble oxyanion tellurite, TeO_3^{-2}, is thought to be due to its strong oxidizing effects on many enzymatic processes (Summers and Jacoby, 1977) and its ability to replace sulfur in metabolic reactions (Turner et al., 1995).

Tellurite resistance in bacteria

Although bacteria rarely come into contact with tellurium, with the exception of highly polluted environments, there are several different and seemingly unrelated tellurite resistance

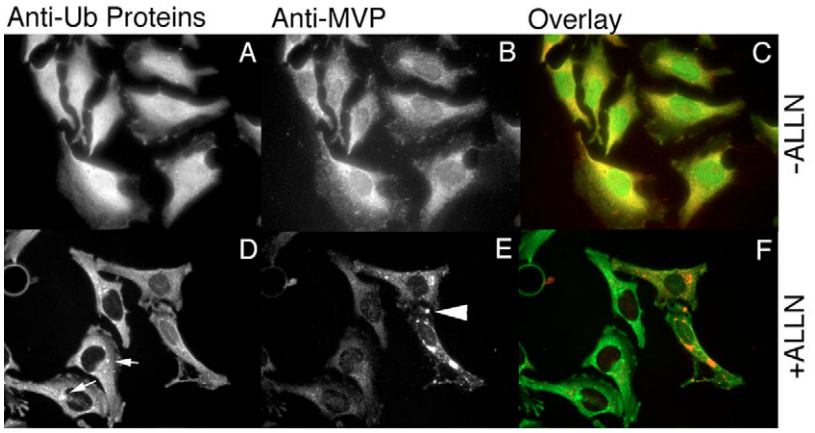

Fig. 7. Aggresomes and vaultosomes are distinct cytosolic entities. HeLa cells were incubated in the presence (D–F) and absence (A–C) of 10 mg ml^{-1} ALLN for 12 h and then processed for immunofluorescence with the FK2 antibodies against ubiquinated proteins (Ub) (A,D) or antibodies against MVP (B,E). Three color overlays are shown in C and F.

(Te^R) determinants that are found both on plasmids and in the genomes of unrelated bacteria (Taylor, 1999). In general, bacterial Te^R does not involve active efflux or reduced uptake of tellurium compounds, but rather the conversion of tellurite to a form that is less toxic to the bacteria. Some determinants involve basic cysteine metabolism (O'Gara et al., 1997) or methyl group transfer (Cournoyer et al., 1998) to detoxify tellurite. In *E. coli*, a basal level of tellurite resistance is brought about by nitrate reductase enzymes that are able to reduce tellurite and selenate at the cell membrane (Avazeri et al., 1997). In addition, the thiol:redox buffering system (glutathione and thioredoxin) appears to play an important role. One of the targets for tellurite toxicity in *E. coli* as well as erythrocyes is glutathione (Deuticke et al., 1992; Turner et al., 2001; Young et al., 1981). However, at this time there is no unifying theory of tellurite resistance. In this regard, tellurite resistance is thought to be a secondary effect of a normal metabolic or stress response pathway (Taylor, 1999).

The photosynthetic bacteria, *Rhodobacter sphaeroides* strain 2.4.1, has a surprising metabolic repertoire that includes anaerobic photosynthesis, aerobic and anaerobic respiration, as well as nitrogen and carbon fixation. *R. sphaeroides* survives in high levels of rare-earth oxides and oxyanions such as tellurite and selenite (Moore and Kaplan, 1992). Te^R in *R. sphaeroides* 2.4. is associated with two loci, *trgAB* and *telA* (O'Gara et al., 1997). The *trgAB* genes confer Te^R when introduced into the related bacterium *Paracoccus denitrificans*. In addition, a TelA null strain shows a partial decrease in resistance when compared to a wild-type strain. The mechanism of TrgAB and TelA associated resistance remains unknown.

The TelA protein family

The toxic anion resistance protein (TelA) family consists of several prokaryotic TelA-like proteins including the TelA protein of *R. sphaeroides*, *D. radiodurans*, *B. subtilis* and *Y. pestis* (O'Gara et al., 1997), the KIA protein associated with plasmid fertility inhibition (Whelan et al., 1995) and the KlaA protein from the methanomicrobe, *Methanosarcina acetivorans*.

In this report, we have shown that the eukaryotic major vault protein also shares significant sequence similarity with the TelA protein of *Rhodobacter sphaeroides*, and make a reasonable argument that the two share a common fold, spatial size and shape, and electrostatic profile. A solution NMR structure reveals a unique, novel fold consisting of a three-stranded antiparallel β-sheet (Kozlov et al., 2006). Our molecular modeling of the bacterial TelA protein reveals a common fold. Further evidence for a common MVP and TelA ancestry was obtained when it was shown that the MVP repeat segment and the TelA protein display greater than 60% similarity with S-layer paracrystalline bacterial surface coatings. These results indicate that the TelA protein may be a distant relative of the major vault protein.

In bacterial cells, it has been speculated that tellurite resistance is not the primary property of any of the unrelated tellurite resistance determinants (Taylor, 1999). The lack of similarity between any of the proteins associated with tellurite resistance has confounded their functional analysis. In addition, most bacteria rarely encounter high levels of tellurite in their environment so it is difficult to understand why so many bacteria maintain these genes in their genomes and on plasmids. If the primary function of the Te^R proteins is not to confer tellurite resistance why have they been conserved amongst so many divergent bacteria?

An intriguing hypothesis was put forth (Taylor, 1999) that the primary role of the Te^R determinants might be to protect the bacterium from mammalian host defenses. Many pathogenic bacteria are resistant to tellurite and one or more Te^R determinants have been identified in *Y. pestis*, *M. tuberculosis* and *N. meningitidis*, for example. In Taylor's model, the products of the Te^R genes are able to counterattack toxic substances produced by macrophages and other human cellular defenses. It is curious that mammalian vaults are very abundant in macrophages and in the dendritic cells of the immune system (Mossink et al., 2003; Mossink et al., 2002; Schroeijers et al., 2002). It is intriguing to speculate that macrophages inherited a tellurite-resistant gene from an ancestral pathogen and that vaults are an unrealized component of a metabolic pathway that originated in bacteria.

Vault function?

Movement of vaults to the cell surface in response to tellurite suggests that there is a link between MVP and the TelA protein. In response to a sublethal dose of K_2TeO_3, large vault aggregates appear at the cell margins. Aggregate formation is dynamic and reversible and occurs in normal cells grown in

culture as well as cancer cell lines. Vaultosomes form independently of stress granules and from aggresomes.

Curiously, vaultosomes were induced by treatment of cells with ALLN, which is an inhibitor of neutral cysteine proteases. This result suggests that thiol-modified proteins may accumulate in the vicinity of vaultosomes and that vaults may be involved in the complex biochemical sensing and response to perturbations in the thiol:redox buffering system. It has been known for quite some time that selenium and tellurium compounds are thiol reactive reagents and all of these oxyanions perturb the thiol:redox buffering system (Bersin and Logemann, 1933; Valko et al., 2006). Our study shows that vaults respond dynamically to these toxic oxyanions. The large size of the vault interior indicates that vaults could harbor macromolecular complexes at the cell surface in response to tellurite uptake. Recent work shows that the vault shell can open and close transiently (Poderycki et al., 2006). Whether vaults contain complexes of organic telluroproteins (Ramadan et al., 1989), macromolecular complexes involved in the reduction of tellurite to elemental tellurium (Deuticke et al., 1992; Turner et al., 1992), or components of the thiol:redox system remains to be determined.

List of abbreviations

ALLN	N-acetyl-Leu-Leu-Norleucinal
CHARMM	Chemistry at HARvard Molecular Mechanics
ERKs	extracellular regulated kinases
HUVEC	human umbilical vascular endothelial
MDR	multidrug resistant
MVP	major vault protein
NMR	nuclear magnetic resonance
PSI-BLAST	position specific iterated basic local alignment search tool
TelA	toxic anion (tellurite) resistance protein
TEP1	telomerase-associated protein
VPARP	vault poly(ADP-ribose) polymerase

This project was supported by NSF MCB-9982377 and NIH Grants Numbers P20 RR015563 and P20 RR016475 from the COBRE and INBRE Programs of the National Center for Research Resources, with matching support from the State of Kansas, and the University of Kansas. N.B. was supported by the NSF Research Experiences for Undergraduates Program.

References

Altschul, S. F. and Koonin, E. V. (1998). Iterated profile searches with PSI-BLAST – a tool for discovery in protein databases. *Trends Biochem. Sci.* **23**, 444-447.

Anderson, P. and Kedersha, N. (2002). Stressful initiations. *J. Cell Sci.* **115**, 3227-3234.

Avazeri, C., Turner, R. J., Pommier, J., Weiner, J. H., Giordano, G. and Vermeglio, A. (1997). Tellurite reductase activity of nitrate reductase is responsible for the basal resistance of *Escherichia coli* to tellurite. *Microbiology* **143**, 1181-1189.

Bersin, T. and Logemann, W. (1933). Mercaptides of selenium and tellurium. *Liebigs Ann. Chem.* **505**, 1-16.

Chugani, D. C., Rome, L. H. and Kedersha, N. L. (1993). Evidence that vault ribonucleoprotein particles localize to the nuclear pore complex. *J. Cell Sci.* **106**, 23-29.

Cooper, W. C. (1971). *Tellurium*. New York: Van Nostrand Reinhold.

Cournoyer, B., Watanabe, S. and Vivian, A. (1998). A tellurite-resistance genetic determinant from phytopathogenic pseudomonads encodes a thiopurine methyltransferase: evidence of a widely conserved family of methyltransferases. *Biochim. Biophys. Acta* **1397**, 161-168.

Deuticke, B., Lutkemeier, P. and Poser, B. (1992). Tellurite-induced damage of the erythrocyte membrane. Manifestations and mechanisms. *Biochim. Biophys. Acta* **1109**, 97-107.

Ding, W. J., Hasegawa, T., Peng, D., Hosaka, H. and Seko, Y. (2002). Preliminary investigation on the cytotoxicity of tellurite to cultured HeLa cells. *J. Trace Elem. Med. Biol.* **16**, 99-102.

Dreyfuss, G., Matunis, M. J., Pinol-Roma, S. and Burd, C. G. (1993). hnRNP proteins and the biogenesis of mRNA. *Annu. Rev. Biochem.* **62**, 289-321.

Eichenmuller, B., Kedersha, N., Solovyeva, E., Everley, P., Lang, J., Himes, R. H. and Suprenant, K. A. (2003). Vaults bind directly to microtubules via their caps and not their barrels. *Cell Motil. Cytoskel.* **56**, 225-236.

Gorlach, M., Burd, C. G. and Dreyfuss, G. (1994). The mRNA poly(A)-binding protein: localization, abundance, and RNA-binding specificity. *Exp. Cell Res.* **211**, 400-407.

Hamill, D. R. and Suprenant, K. A. (1997). Characterization of the sea urchin major vault protein: a possible role for vault ribonucleoprotein particles in nucleocytoplasmic transport. *Dev. Biol.* **190**, 117-128.

Hamilton, B. J., Nichols, R. C., Tsukamoto, H., Boado, R. J., Pardridge, W. M. and Rigby, W. F. (1999). hnRNP A2 and hnRNP L bind the 3′UTR of glucose transporter 1 mRNA and exist as a complex in vivo. *Biochem. Biophys. Res. Commun.* **261**, 646-651.

Harry, G. J., Goodrum, J. F., Bouldin, T. W., Wagner-Recio, M., Toews, A. D. and Morell, P. (1989). Tellurium-induced neuropathy: metabolic alterations associated with demyelination and remyelination in rat sciatic nerve. *J. Neurochem.* **52**, 938-945.

Henikoff, S. and Henikoff, J. G. (1992). Amino acid substitution matrices from protein blocks. *Proc. Natl. Acad. Sci. USA* **89**, 10915-10919.

Hulo, N., Sigrist, C. J., Le Saux, V., Langendijk-Genevaux, P. S., Bordoli, L., Gattiker, A., De Castro, E., Bucher, P. and Bairoch, A. (2004). Recent improvements to the PROSITE database. *Nucleic Acids Res.* **32**, D134-D137.

Johnston, J. A., Ward, C. L. and Kopito, R. R. (1998). Aggresomes: a cellular response to misfolded proteins. *J. Cell Biol.* **143**, 1883-1898.

Kedersha, N. L., Hill, D. F., Kronquist, K. E. and Rome, L. H. (1986). Subpopulations of liver coated vesicles resolved by preparative agarose gel electrophoresis. *J. Cell Biol.* **103**, 287-297.

Kedersha, N. L., Miquel, M. C., Bittner, D. and Rome, L. H. (1990). Vaults. II. Ribonucleoprotein structures are highly conserved among higher and lower eukaryotes. *J. Cell Biol.* **110**, 895-901.

Kedersha, N. L., Gupta, M., Li, W., Miller, I. and Anderson, P. (1999). RNA-binding proteins TIA-1 and TIAR link the phosphorylation of eIF-2 alpha to the assembly of mammalian stress granules. *J. Cell Biol.* **147**, 1431-1442.

Kedersha, N., Cho, M. R., Li, W., Yacono, P. W., Chen, S., Gilks, N., Golan, D. E. and Anderson, P. (2000). Dynamic shuttling of TIA-1 accompanies the recruitment of mRNA to mammalian stress granules. *J. Cell Biol.* **151**, 1257-1268.

Kickhoefer, V. A., Siva, A. C., Kedersha, N. L., Inman, E. M., Ruland, C., Streuli, M. and Rome, L. H. (1999). The 193-kD vault protein, VPARP, is a novel poly(ADP-ribose) polymerase. *J. Cell Biol.* **146**, 917-928.

Kolli, S., Zito, C. I., Mossink, M. H., Wiemer, E. A. and Bennett, A. M. (2004). The major vault protein is a novel substrate for the tyrosine phosphatase SHP-2 and scaffold protein in epidermal growth factor signaling. *J. Biol. Chem.* **279**, 29374-29385.

Kong, L. B., Siva, A. C., Rome, L. H. and Stewart, P. L. (1999). Structure of the vault, a ubiquitous celular component. *Structure* **7**, 371-379.

Kozlov, G., Vavelyuk, O., Minailiuc, O., Banville, D., Gehring, K. and Ekiel, I. (2006). Solution structure of a two-repeat fragment of major vault protein. *J. Mol. Biol.* **356**, 444-452.

Kwon, S., Barbarese, E. and Carson, J. H. (1999). The cis-acting RNA trafficking signal from myelin basic protein mRNA and its cognate trans-acting ligand hnRNP A2 enhance cap-dependent translation. *J. Cell Biol.* **147**, 247-256.

Lampert, P., Garro, F. and Pentschew, A. (1970). Tellurium neuropathy. *Acta Neuropathol.* **15**, 308-317.

Laskowski, R. A., MacArthur, M. W., Moss, D. S. and Thornton, J. M. (1993). PROCHECK: a program to check the stereochemical quality of protein structures. *J. Appl. Cryst.* **2**, 283-291.

MacKerell, A. D., Jr, Brooks, B., Brooks, C. B., III, Nilsson, L., Roux, B., Won, Y. and Karplus, M. (1998). CHARMM: The energy function and its parameterization with an overview of the program. In *Encyclopedia of Computational Chemistry*. Vol. 1 (ed. P. von Ragué Schleyer, N. L. Allinger, T. Clark, J. Gasteiger, P. A. Kollman, H. F. Schaefer, III and P. R. Schreiner), pp. 271-277. Chichester: John Wiley and Sons.

Marti-Renom, M. A., Stuart, A. C., Fiser, A., Sanchez, R., Melo, F. and Sali, A. (2000). Comparative protein structure modeling of genes and genomes. *Annu. Rev. Biophys. Biomol. Struct.* **29**, 291-325.

Mikyas, Y., Makabi, M., Raval-Fernandes, S., Harrington, L., Kickhoefer, V. A., Rome, L. H. and Stewart, P. L. (2004). Cryoelectron microscopy imaging of recombinant and tissue derived vaults: localization of the MVP N termini and VPARP. *J. Mol. Biol.* **344**, 91-105.

Moore, M. D. and Kaplan, S. (1992). Identification of intrinsic high-level resistance to rare-earth oxides and oxyanions in members of the class Proteobacteria: characterization of tellurite, selenite, and rhodium sesquioxide reduction in *Rhodobacter sphaeroides*. *J. Bacteriol.* **174**, 1505-1514.

Mossink, M. H., van Zon, A., Franzel-Luiten, E., Schoester, M., Kickhoefer, V. A., Scheffer, G. L., Scheper, R. J., Sonneveld, P. and Wiemer, E. A. (2002). Disruption of the murine major vault protein (MVP/LRP) gene does not induce hypersensitivity to cytostatics. *Cancer Res.* **62**, 7298-7304.

Mossink, M. H., de Groot, J., van Zon, A., Franzel-Luiten, E., Schoester, M., Scheffer, G. L., Sonneveld, P., Scheper, R. J. and Wiemer, E. A. (2003). Unimpaired dendritic cell functions in MVP/LRP knockout mice. *Immunology* **110**, 58-65.

Nichols, R. C., Wang, X. W., Tang, J., Hamilton, B. J., High, F. A., Herschman, H. R. and Rigby, W. F. (2000). The RGG domain in hnRNP A2 affects subcellular localization. *Exp. Cell Res.* **256**, 522-532.

O'Gara, J. P., Gomelsky, M. and Kaplan, S. (1997). Identification and molecular genetic analysis of multiple loci contributing to high-level tellurite resistance in *Rhodobacter sphaeroides* 2.4.1. *Appl. Environ. Microbiol.* **63**, 4713-4720.

Poderycki, M. J., Kickhoefer, V. A., Kaddis, C. S., Raval-Fernandes, S., Johansson, E., Zink, J. I., Loo, J. A. and Rome, L. H. (2006). The vault exterior shell is a dynamic structure that allows incorporation of vault-associated proteins into its interior. *Biochemistry* **45**, 12184-12193.

Ramadan, S. E., Razak, A. A., Ragab, A. M. and el-Meleigy, M. (1989). Incorporation of tellurium into amino acids and proteins in a tellurium-tolerant fungi. *Biol. Trace Elem. Res.* **20**, 225-232.

Scheffer, G. L., Schroeijers, A. B., Izquierdo, M. A., Wiemer, E. A. and Scheper, R. J. (2000). Lung resistance-related protein/major vault protein and vaults in multidrug-resistant cancer. *Curr. Opin. Oncol.* **12**, 550-556.

Schroeijers, A. B., Reurs, A. W., Scheffer, G. L., Stam, A. G., de Jong, M. C., Rustemeyer, T., Wiemer, E. A., de Gruijl, T. D. and Scheper, R. J. (2002). Up-regulation of drug resistance-related vaults during dendritic cell development. *J. Immunol.* **168**, 1572-1578.

Siva, A. C., Raval-Fernandes, S., Stephen, A. G., LaFemina, M. J., Scheper, R. J., Kickhoefer, V. A. and Rome, L. H. (2001). Up-regulation of vaults may be necessary but not sufficient for multidrug resistance. *Int. J. Cancer* **92**, 195-202.

Slesina, M., Inman, E. M., Rome, L. H. and Volknandt, W. (2005). Nuclear localization of the major vault protein in U373 cells. *Cell Tissue Res.* **321**, 97-104.

Steiner, E., Holzmann, K., Pirker, C., Elbling, L., Micksche, M., Sutterluty, H. and Berger, W. (2006). The major vault protein is responsive to and interferes with interferon-gamma-mediated STAT1 signals. *J. Cell Sci.* **119**, 459-469.

Stephen, A. G., Raval-Fernandes, S., Huynh, T., Torres, M., Kickhoefer, V. A. and Rome, L. H. (2001). Assembly of vault-like particles in insect cells expressing only the major vault protein. *J. Biol. Chem.* **276**, 23217-23220.

Stewart, P. L., Makabi, M., Lang, J., Dickey-Sims, C., Robertson, A. J., Coffman, J. A. and Suprenant, K. A. (2005). Sea urchin vault structure, composition, and differential localization during development. *BMC Dev. Biol.* **5**, 3.

Summers, A. O. and Jacoby, G. A. (1977). Plasmid-determined resistance to tellurium compounds. *J. Bacteriol.* **129**, 276-281.

Suprenant, K. A. (2002). Vault ribonucleoprotein particles: sarcophagi, gondolas, or safety deposit boxes? *Biochemistry* **41**, 14447-14454.

Taupin, J. L., Tian, Q., Kedersha, N., Robertson, M. and Anderson, P. (1995). The RNA-binding protein TIAR is translocated from the nucleus to the cytoplasm during Fas-mediated apoptotic cell death. *Proc. Natl. Acad. Sci. USA* **92**, 1629-1633.

Taylor, D. E. (1999). Bacterial tellurite resistance. *Trends Microbiol.* **7**, 111-115.

Thompson, J. D., Higgins, D. G. and Gibson, T. J. (1994). CLUSTAL W: improving the sensitivity of progressive multiple sequence alignment through sequence weighting, position-specific gap penalties and weight matrix choice. *Nucleic Acids Res.* **22**, 4673-4680.

Tripos (2006). *SYBYL 7.1*. St Louis, MO: The Tripos Associates.

Turner, R. J., Hou, Y., Weiner, J. H. and Taylor, D. E. (1992). The arsenical ATPase efflux pump mediates tellurite resistance. *J. Bacteriol.* **174**, 3092-3094.

Turner, R. J., Weiner, J. H. and Taylor, D. E. (1995). The tellurite-resistance determinants tehAtehB and klaAklaBtelB have different biochemical requirements. *Microbiology* **141**, 3133-3140.

Turner, R. J., Aharonowitz, Y., Weiner, J. H. and Taylor, D. E. (2001). Glutathione is a target in tellurite toxicity and is protected by tellurite resistance determinants in *Escherichia coli*. *Can. J. Microbiol.* **47**, 33-40.

Valko, M., Rhodes, C. J., Moncol, J., Izakovic, M. and Mazur, M. (2006). Free radicals, metals and antioxidants in oxidative stress-induced cancer. *Chem. Biol. Interact.* **160**, 1-40.

van Zon, A., Mossink, M. H., Schoester, M., Scheffer, G. L., Scheper, R. J., Sonneveld, P. and Wiemer, E. A. (2002). Structural domains of vault proteins: a role for the coiled coil domain in vault assembly. *Biochem. Biophys. Res. Commun.* **291**, 535-541.

van Zon, A., Mossink, M. H., Schoester, M., Houtsmuller, A. B., Scheffer, G. L., Scheper, R. J., Sonneveld, P. and Wiemer, E. A. (2003). The formation of vault-tubes: a dynamic interaction between vaults and vault PARP. *J. Cell Sci.* **116**, 4391-4400.

van Zon, A., Mossink, M. H., Houtsmuller, A. B., Schoester, M., Scheffer, G. L., Scheper, R. J., Sonneveld, P. and Wiemer, E. A. (2006). Vault mobility depends in part on microtubules and vaults can be recruited to the nuclear envelope. *Exp. Cell Res.* **312**, 245-255.

Whelan, K. F., Colleran, E. and Taylor, D. E. (1995). Phage inhibition, colicin resistance, and tellurite resistance are encoded by a single cluster of genes on the IncHI2 plasmid R478. *J. Bacteriol.* **177**, 5016-5027.

Wojcik, C., Schroeter, D., Wilk, S., Lamprecht, J. and Paweletz, N. (1996). Ubiquitin-mediated proteolysis centers in HeLa cells: indication from studies of an inhibitor of the chymotrypsin-like activity of the proteasome. *Eur. J. Cell Biol.* **71**, 311-318.

Young, J. D., Crowley, C. and Tucker, E. M. (1981). Haemolysis of normal and glutathione-deficient sheep erythrocytes by selenite and tellurite. *Biochem. Pharmacol.* **30**, 2527-2530.